

Bioactive *ent*-Kaurane Diterpenoids from *Isodon rosthornii*

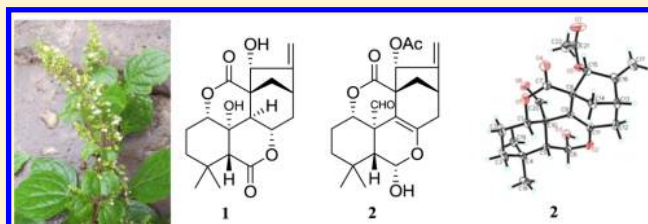
Rui Zhan,^{†,‡} Xiao-Nian Li,[†] Xue Du,[†] Wei-Guang Wang,[†] Ke Dong,[†] Jia Su,[†] Yan Li,[†] Jian-Xin Pu,^{*,†} and Han-Dong Sun^{*,†}

[†]State Key Laboratory of Phytochemistry and Plant Resources in West China, Kunming Institute of Botany, Chinese Academy of Sciences, Kunming 650204, People's Republic of China

[‡]University of Chinese Academy of Sciences, Beijing 100039, People's Republic of China

Supporting Information

ABSTRACT: Isorosthin A (**1**), the first 20-*nor*-*ent*-nein-type diterpenoid, and 15 new *ent*-kauranoids, isorosthins B–P (**2**–**16**), along with 22 known analogues were isolated from the aerial parts of *Isodon rosthornii*. The structures of **1**–**16** were elucidated by means of spectroscopic analysis. The relative configuration of **2** and the absolute configuration of **3** were determined by single-crystal X-ray diffraction. Cytotoxicity evaluation against five human tumor lines showed inhibitory effects by several of the compounds tested. Furthermore, 12 of the isolates exhibited inhibitory activity against nitric oxide production in LPS-activated RAW264.7 macrophages.



Isodon is a cosmopolitan and important genus of the family Lamiaceae, and the use of *Isodon* species in Chinese folk medicine has had a long history.¹ Phytochemical investigation of this genus has confirmed that it is an abundant source of diterpenoids (mainly *ent*-kauranoids), of which some have exhibited a broad spectrum of biological activities, including antibacterial, antitumor, and anti-inflammatory effects, and a direct stimulatory action on osteoblast differentiation.^{1,2} Several purified *ent*-kauranoids have potential anticancer activity, such as eriocalyxin B,^{3,4} pharicin A,⁵ pharicin B,⁶ oridonin,⁷ ponidicin,⁸ and adenanthin.⁹

Isodon rosthornii (Diels) Hara (Lamiaceae), a perennial herb used to treat rheumatism and sore throats, has not been subjected to extensive phytochemical work before.^{10–13} A sample of this plant collected in Sichuan Province, People's Republic of China, afforded three *ent*-kauranoids.¹⁴ Further work on this sample has now been conducted in the present investigation. After pretreatment of the EtOAc-solubles, the combined use of semi-HSCCC and HPLC enabled the isolation of 16 new *ent*-kaurane diterpenoids and 22 known analogues. Reported herein are the isolation, structural elucidation, and biological evaluation of these compounds.

RESULTS AND DISCUSSION

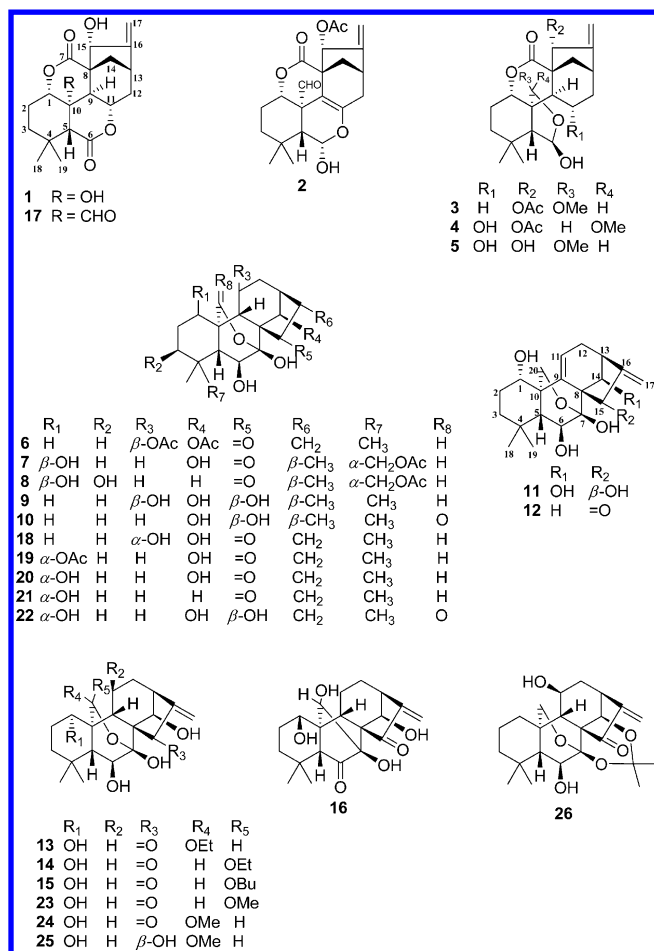
A 70% aqueous acetone extract of the air-dried and powdered aerial parts of *I. rosthornii* was partitioned between EtOAc and H₂O. The EtOAc extract was subjected to column chromatography over silica gel, MCI CHP-20 gel, Sephadex LH-20, and Lichroprep RP-18 and was further purified by semipreparative HSCCC and semipreparative HPLC to afford 16 new *ent*-kaurane diterpenoids, which have been named isorosthins A–P (**1**–**16**), and 22 known compounds. The structures of these known compounds were determined by comparing their

spectroscopic data with literature values, and they were identified as 15 α -hydroxy-6,7-*seco*-1 α ,7:11 α ,6-diolide-*ent*-kaur-16-ene (**17**),¹⁵ longikaurin G (**18**),¹⁶ lasiakaurin (**19**),¹⁷ isodonol (**20**),¹⁸ effusanin A (**21**),¹⁹ rabdoternin B (**22**),²⁰ rabdoternin F (**23**),²¹ rabdoternin E (**24**),²¹ rubescensin O (**25**),²² 7 α ,20-epoxy-6 β ,11 β -dihydroxy-7 β ,14 β -[(1-methylethylidene)-bis-oxy]-*ent*-kaur-16-en-15-one (**26**),²³ 15 α ,20 β -dihydroxy-6 β -methoxy-6,7-*seco*-6,20-epoxy-1,7-olide-*ent*-kaur-16-ene,²⁴ glaucocalactone,²⁵ isodonhenrin B,²⁶ 6 α ,15 α -dihydroxy-20-aldehyde-6,7-*seco*-6,11 α -epoxy-1,7-olide-*ent*-kaur-16-ene,¹⁶ sculponeatin E,²⁷ rosthornin A,¹⁰ lasiakaurinol,²¹ rabdoternin A,²¹ hebeirubescensin H,²⁸ isoadenolin E,²⁹ rubescensin D,³⁰ and phyllostachysin A.³¹

Compound **1** was obtained as a white, amorphous powder. The HRESIMS of **1** exhibited a [M + Na]⁺ peak at 371.1481, which suggested a molecular formula of C₁₉H₂₄O₆, indicating eight degrees of unsaturation. Its IR spectrum gave absorption bands at 3432, 1724, and 1630 cm⁻¹, accounting for the presence of OH, C=O, and C=C groups. Assignments of the ¹H and ¹³C NMR spectra of **1** (Tables 1 and 2) were supported by a series of 2D-NMR (¹H–¹H COSY, HSQC, HMBC) experiments. In the ¹³C NMR and DEPT spectra (Table 2), 19 carbon signals were observed, which were assigned as two methyls, five methylenes (including one olefinic), six methines (of which three are oxygenated), and six quaternary carbons (including two carbonyls, one olefinic and one oxygenated). These data indicated that **1** is a *nor*-6,7-*seco*-1,7:6,11-diolide-*ent*-kauranoid, similar to compound **17**.¹⁵ Analysis of its ¹H–¹H COSY, HSQC, and HMBC spectra confirmed this assumption and helped furnish the planar structure of compound **1**. HMBC

Received: March 5, 2013

Published: July 2, 2013



correlations (Figure 1) from H₂-17 (δ_{H} 5.53 and 5.21) and H-13 (δ_{H} 2.86) to C-15 (δ_{C} 81.2) permitted the location of an OH group at C-15. Correlations from H-1 (δ_{H} 4.62) and H-11 (δ_{H} 4.83) to C-10 (δ_{C} 70.9), along with the comparison of the chemical shift value of C-10 in **1** with that in **17** (δ_{C} 50.8) showed that C-10 is oxygenated. According to the molecular formula, the OH group was coupled to C-10 directly.

On biogenetic grounds, compound **1** was confirmed as an *ent*-kauranoid with the configuration of H-5 being β -oriented. ROESY correlations from H-1 to H-5 β , H-11 to H-5 β , and H-15 to H-14 α revealed H-1, H-11, and H-15 also to be β -oriented. In turn, a correlation between HO-10 and H-9 α showed that HO-10 is α -oriented (Figure 1). Thus, compound **1** was elucidated as 10 α ,15 α -dihydroxy-6,7-*seco*-1 α ,7:6,11 α -diolide-20-*nor-ent*-kaur-16-ene and is the first 20-*nor*-enmein-type diterpenoid to have been reported.

Compound **2** was obtained as colorless needles when crystallized from a mixed solvent system (petroleum ether–acetone, 1:1), with its molecular formula of C₂₂H₂₆O₇ determined by HRESIMS ($[\text{M} + \text{Na}]^+$ m/z 425.1578, calcd 425.1576). Its IR spectrum revealed the presence of OH, C=O, and C=C groups from absorptions at 3473, 1740, and 1674 cm⁻¹, respectively. The ¹³C NMR and DEPT spectroscopic data (Table 2) exhibited 22 carbon signals, including an acetyl group, two methyls, five methylenes (one olefinic), six methines (three oxygenated and one aldehyde carbon), and seven quaternary carbons (three olefinic and one carbonyl carbon). Detailed analysis of the NMR spectra (Tables 1 and 2) indicated that **2** is also a 6,7-*seco*-1,7-olide-*ent*-kauranoid, but contains two double bonds in its structure. One of these is a

terminal double bond between C-16 and C-17, and the other was placed at the junction of rings B and D from the key correlations in the HMBC spectrum, from H-1 (δ_{H} 5.07), H-5 (δ_{H} 1.62), H-12 (δ_{H} 2.15), and H-15 (δ_{H} 6.17) to C-9 (δ_{C} 102.2) and from H-13 (δ_{H} 3.11) and H-12 (δ_{H} 2.15 and 2.58) to C-11 (δ_{C} 146.7) (Figure 2). HMBC correlations from H-5 to C-6 (δ_{C} 91.6) and from H-6 (δ_{H} 6.17) to C-11 were consistent with the presence of a hemiacetal ring linking C-6 to C-11 (Figure 2). Correlations from H-15 to the carbonyl carbon of the OAc (δ_{C} 170.0) permitted the location of an acetyl group at C-15, and correlations from H-20 (δ_{H} 9.98) to C-10 and from H-5 and H-1 to C-20 supported the location of the CHO group at C-10. The relative configurations of H-1, H-6, and H-15 were confirmed as all β -oriented by the ROESY correlations of H-1/H-3 β /H-5 β , H-6/H-5 β /H₃-18 β , and H-15/H-14 α (Figure 2). Finally, an X-ray crystallographic experiment (Figure 3) was used to confirm that the structure of **2** is 15 α -acetoxy-6 α -hydroxy-20-oxo-6,11-epoxy-6,7-*seco*-1 α ,7-olide-*ent*-kaur-9-(11),16-diene.

Compound **3** was obtained as colorless crystals that gave a molecular formula of C₂₃H₃₂O₇, as deduced by HRESIMS. Comparison of the NMR data of **3** with those of 15 α ,20 β -dihydroxy-6 β -methoxy-6,7-*seco*-6,20-epoxy-1,7-olide-*ent*-kaur-16-ene suggested that these two compounds are similar structurally²⁴ and indicated the replacement of the C-6 OMe, C-15 OH, and C-20 OH groups in the known compound by hydroxy, acetate, and methoxy functionalities, respectively, in **3** (Figure 4). These inferences were confirmed by 2D-NMR experiments. Furthermore, a single crystal of **3** was afforded from the solvent system CH₃OH–pyridine (10:1) and analyzed by X-ray crystallography. Compound **3** had seven oxygen atoms in the molecule, and the final refinement on Cu K α data resulted in a Flack parameter of 0.02(12),³² allowing an unambiguous assignment of its complete absolute configuration as shown (Figure 5). All chiral centers, C-1, C-5, C-6, C-8, C-9, C-10, C-13, C-15, and C-20, were determined as *S*, *R*, *R*, *S*, *R*, *R*, *R*, *R*, and *R*, respectively. Therefore, compound **3** was determined as 20(*R*)-15 α -acetoxy-6 β -hydroxy-20-methoxy-6,20 α -epoxy-6,7-*seco*-1 α ,7-olide-*ent*-kaur-16-ene.

Compound **4**, with a molecular formula of C₂₃H₃₂O₈ confirmed by HRESIMS, exhibited similar NMR data to **3** (Tables 1 and 2). The connectivity of an additional OH group to C-11 in **4** was confirmed by HMBC correlations from H-9 (δ_{H} 3.79) and H-13 (δ_{H} 2.66) to C-11 (δ_{C} 62.3) and from H-11 (δ_{H} 4.33) to C-10 (δ_{C} 50.9). ROESY correlations of H-1/H-3 β /H-5 β , H-6/H₃-19 α , H-11/H-5 β /H-1 β , and H-15/H-14 α supported the configurations of H-1, H-6, H-11, and H-15 as being β -, α -, β -, and β -oriented, respectively. The relative configuration of C-20 was assigned as *S** from the ROESY correlation of H-20 and H₃-19 α . Consequently, compound **4** was assigned as 20(*S**)-15 α -acetoxy-6 β ,11 α -dihydroxy-20-methoxy-6,20 α -epoxy-6,7-*seco*-1 α ,7-olide-*ent*-kaur-16-ene.

Comparison of the spectroscopic data of compound **5** with those of **4** (Tables 1 and 2) demonstrated the substitution of the OAc group in **4** by an OH group in **5**. 2D-NMR spectra were used to verify the structure of **5** and revealed that the relative configurations of H-1, H-6, and H-15 in **5** are the same as those of **4**. However, the relative configuration of C-20 in **5** was indicated as *R** by the correlation of H-20 and H-9 α in its ROESY spectrum. Compound **5** was thus established as 20(*R**)-6 β ,11 α ,15 α -trihydroxy-20-methoxy-6,20 α -epoxy-6,7-*seco*-1 α ,7-olide-*ent*-kaur-16-ene.

Table 1. ¹H NMR Spectroscopic Data for Isorosthins A–E (1–5) (δ in ppm, J in Hz)

position	1 ^{a,c}	2 ^{b,c}	3 ^{a,c}	4 ^{a,c}	5 ^{a,c}
1	4.62, dd (11.6, 3.7)	4.00, dd (12.4, 4.0)	4.69, dd (11.4, 5.9)	4.86, m	4.81, dd (11.5, 5.8)
2a	2.63, overlap	2.22, overlap	2.42, m	1.94, overlap	2.47, m
2b	1.96, m	2.07, overlap	1.81, m		1.88, m
3a	1.59, m	1.64, overlap	1.48, overlap	1.46, m	1.45, m
3b	1.48, m	1.43, m	1.26, overlap	1.38, m	1.31, m
5	2.79, brs	1.62, overlap	2.24, brs	3.13, brs	3.22, brs
6		5.61, d (2.4)	5.91, brs	5.59, d (4.0)	5.84, d (7.0)
9	3.28, d (11.9)		3.09, dd (12.6, 5.3)	3.79, d (9.5)	3.33, d (9.6)
11a	4.83, m		2.13, overlap	4.33, m	4.41, m
11b			1.43, overlap		
12a	2.66, overlap	2.58, dd (16.7, 4.6)	2.12, overlap	2.93, m	2.96, m
12b	1.71, m	2.15, overlap	1.52, overlap	1.94, overlap	1.88, m
13	2.86, m	3.11, m	2.63, m	2.66, m	2.74, m
14a	2.16, d (12.2)	2.34, dd (11.2, 5.3)	2.12, overlap	2.24, d (12.0)	1.76, m
14b	1.83, dd (12.2, 4.8)	1.92, d (11.2)	1.70, m	1.60, d (12.0)	2.10, d (11.8)
15	5.71, s	6.17, s	6.66, s	7.07, s	5.74, s
17a	5.53, s	5.15, s	5.01, overlap	5.13, s	5.55, s
17b	5.21, s	5.05, s	5.01, overlap	5.06, s	5.27, s
18	1.28, s	1.08, s	1.07, s	1.09, s	1.08, s
19	1.78, s	1.00, s	1.24, s	1.02, s	1.27, s
20		9.98, s	5.24, s	5.37, s	5.57, s
HO-6				9.22, s	
HO-10	7.75, s				
HO-11				7.52, s	
HO-15	8.27, s				
OAc		2.13, s		2.11, s	
OMe			3.43, s	3.44, s	3.25, s

^aRecorded in C₅D₅N. ^bRecorded in CDCl₃. ^cRecorded at 500 MHz.

Table 2. ¹³C NMR Spectroscopic Data for Isorosthins A–E (1–5) (δ in ppm)

position	1 ^{a,e}	2 ^{b,c}	3 ^{a,d}	4 ^{a,c}	5 ^{a,e}
1	78.9, CH	83.1, CH	76.1, CH	75.8, CH	77.1, CH
2	25.2, CH ₂	25.1, CH ₂	25.2, CH ₂	24.0, CH ₂	25.9, CH ₂
3	40.5, CH ₂	40.6, CH ₂	37.7, CH ₂	37.3, CH ₂	38.5, CH ₂
4	33.9, C	33.2, C	31.2, C	31.7, C	32.2, C
5	53.8, CH	52.2, CH	54.3, CH	54.6, CH	54.0, CH
6	171.2, C	91.6, CH	101.6, CH	99.3, CH	103.0, CH
7	174.6, C	171.9, C	174.4, C	173.4, C	175.6, C
8	50.7, C	49.4, C	52.4, C	53.6, C	54.1, C
9	46.8, CH	102.2, C	39.4, CH	41.7, CH	46.0, CH
10	70.9, C	48.8, C	52.4, C	50.9, C	53.7, C
11	71.4, CH	146.7, C	18.4, CH ₂	62.3, CH	63.6, CH
12	37.9, CH ₂	39.1, CH ₂	32.1, CH ₂	42.3, CH ₂	46.0, CH ₂
13	38.0, CH	39.1, CH	37.5, CH	37.9, CH	37.4, CH
14	32.2, CH ₂	38.8, CH ₂	33.9, CH ₂	35.4, CH ₂	35.2, CH ₂
15	81.2, CH	86.4, CH	79.5, CH	75.9, CH	77.9, CH
16	158.7, C	150.3, C	154.1, C	155.8, C	158.4, C
17	110.1, CH ₂	111.7, CH ₂	109.8, CH ₂	108.5, CH ₂	109.2, CH ₂
18	32.0, CH ₃	29.8, CH ₃	32.3, CH ₃	32.9, CH ₃	34.8, CH ₃
19	22.6, CH ₃	22.8, CH ₃	22.9, CH ₃	23.6, CH ₃	22.8, CH ₃
20		202.4, CH	111.3, CH	109.2, CH	111.2, CH
OAc		20.7, CH ₃	20.8, CH ₃	21.2, CH ₃	
		170.2, C	169.9, C	169.9, C	
OMe			55.6, CH ₃	57.5, CH ₃	55.4, CH ₃

^aRecorded in C₅D₅N. ^bRecorded in CDCl₃. ^cRecorded at 400 MHz. ^dRecorded at 500 MHz. ^eRecorded at 600 MHz.

The spectroscopic characterization of compound **6** indicated it to be a 7,20-epoxy-*ent*-kauranoid, an analogue of rosthornin A (Tables 3 and 4).¹⁰ HRESIMS and 2D-NMR methods were

used to prove the locations of OAc groups at C-11 and C-14, in place of OH-11 and OH-15 in rosthornin A. ROESY correlations of H-6/H₃-19 α , H-11/H-13 α , H-14/H-13 α , and

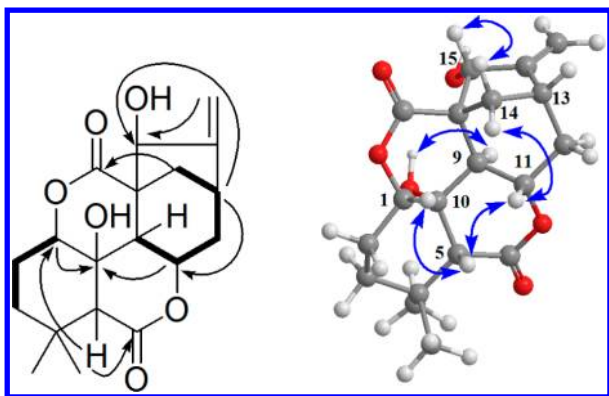


Figure 1. ^1H - ^1H COSY (bold), selected HMBC (arrows), and key ROESY correlations of 1.

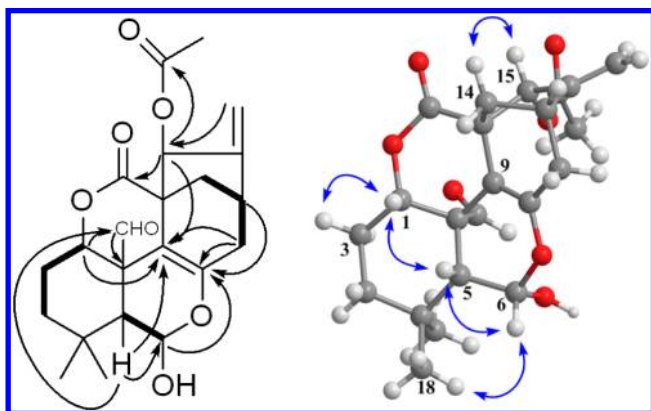


Figure 2. ^1H - ^1H COSY (bold), selected HMBC (arrows), and key ROESY correlations of 2.

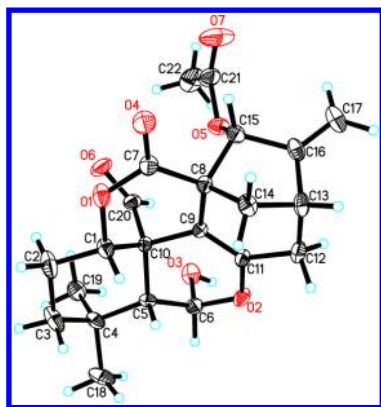


Figure 3. X-ray crystal structure of 2.

H-14/H-11/H-20 revealed H-6, H-11, and H-14 to all be α -oriented. Hence, compound 6 was deduced as 11 β ,14 β -diacetoxy-6 β ,7 β -dihydroxy-7 α ,20-epoxy-*ent*-kaur-16-en-15-one.

The spectroscopic data of compound 7 indicated it to be an analogue of rabdoternin F (Tables 3 and 4),²² with the molecular formula of $\text{C}_{22}\text{H}_{32}\text{O}_8$. The only difference between these two compounds was that the terminal double bond between C-16 and C-17 in rabdoternin F is reduced in 7. From the 2D-NMR spectra, the structure of 7 was confirmed. A ROESY experiment showed that the relative configurations of H-1, H-6, and H-14 in 7 are all α -oriented. The configuration of H-16 was determined as being α -oriented by correlations between H-16/H-14 α and H₃-17/H-12 β . Consequently, 7 was

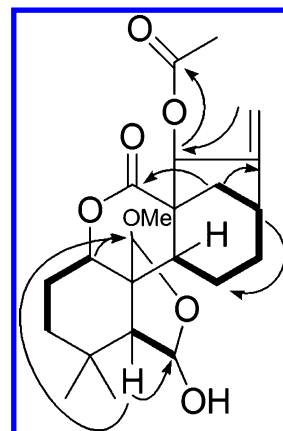


Figure 4. ^1H - ^1H COSY (bold) and selected HMBC (arrows) correlations of 3.

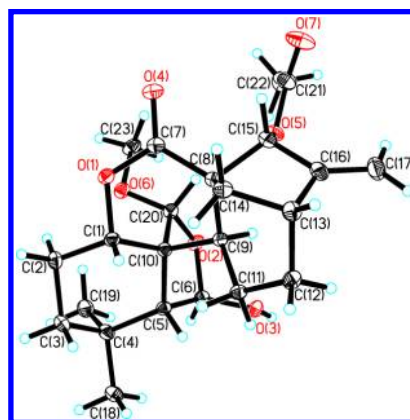


Figure 5. X-ray crystal structure of 3.

elucidated as 19-acetoxy-1 β ,6 β ,7 β ,14 β -tetrahydroxy-7 α ,20-epoxy-*ent*-kaur-15-one.

HRESIMS indicated that compound 8 is an isomer of 7. Careful analysis of the NMR data (Tables 3 and 4) suggested that an OH group is connected to C-3 in 8, instead of the HO-14 group in 7. This assumption was confirmed by HMBC correlations from H-3 (δ_{H} 4.18) to C-18 (δ_{C} 21.8) and C-5 (δ_{C} 52.7). The ROESY spectrum verified that the relative configurations of H-1, H-6, and H-16 in 8 are α -oriented. The relative configuration of H-3 was confirmed as being α -oriented by the correlations of H-3/H-1 α /H₂-19 α . Therefore, compound 8 was deduced as 19-acetoxy-1 β ,3 β ,6 β ,7 β -tetrahydroxy-7 α ,20-epoxy-*ent*-kaur-15-one.

Compound 9, with a molecular formula of $\text{C}_{20}\text{H}_{32}\text{O}_6$, was found to be similar structurally to rosthornin A.¹⁰ Comparison of the NMR data of these two compounds suggested that the α , β -unsaturated ketone in rosthornin A is in a reduced form in 9 (Tables 3 and 4), which was verified by HMBC correlations from H-15 (δ_{H} 5.33) to C-8 (δ_{C} 56.0), C-13 (δ_{C} 36.9), and C-17 (δ_{C} 12.0). The ROESY spectrum was used to determine the configurations of H-6, H-11, H-14, and H-15 as all being α -oriented. The configuration of H-16 was shown to be α -oriented from the correlations of H-16/H-14 α and H₃-17/H-12 β . Thus, compound 9 was assigned as 6 β ,7 β ,11 β ,14 β ,15 β -pentahydroxy-7 α ,20-epoxy-*ent*-kaurane.

The HRESIMS data for compound 10 suggested a molecular formula of $\text{C}_{20}\text{H}_{30}\text{O}_6$. The NMR data showed a close resemblance to those of rabdoternin A (Tables 3 and 4)²¹

Table 3. ¹H NMR Spectroscopic Data for Isorosthins F–J (δ in ppm, J in Hz)

position	6 ^{a,b}	7 ^{a,b}	8 ^{a,b}	9 ^{a,c}	10 ^{a,b}
1a	1.35, overlap	3.64, m	3.69, m	2.02, m	2.29, m
1b	1.20, m			1.84, m	1.27, overlap
2a	1.22–1.28, m	1.82, overlap	2.25, m	1.39, m	1.91, m
2b			2.10, m		1.46, overlap
3a	1.33, overlap	2.06, overlap	4.18, brs	1.33, overlap	1.36, overlap
3b	1.01, m	1.68, m		1.09, overlap	1.15, overlap
5	1.48, overlap	2.34, d (5.2)	2.70, d (5.0)	1.49, d (4.0)	1.63, d (5.0)
6	4.14, overlap	4.41, m	4.49, m	4.16, overlap	4.22, t (4.5)
9	2.11, overlap	2.46, m	2.23, overlap	2.96, d (9.0)	2.90, dd (13.5, 6.5)
11a	5.51, m	2.05, overlap	1.98, m	4.23, overlap	1.40, overlap
11b		1.80, overlap			1.10, overlap
12a	3.25, m	1.83, overlap	1.71, overlap	2.47, dd (14.0, 9.0)	1.77, m
12b	1.50, overlap	1.65, m	1.15, m	2.15, dd (14.0, 9.0)	1.61, m
13	3.15, m	2.56, m	2.33, overlap	3.17, m	2.15, m
14a	6.36, brs	5.27, brs	2.50, dd (11.0, 4.9)	4.97, brs	4.84, brs
14b			2.34, d (11.0)		
15				5.33, d (10.2)	5.71, d (10.2)
16		3.32, m	2.40, m	2.29, m	3.13, m
17a	6.25, brs	1.07, d (7.2)	1.00, d (8.0)	1.28, d (7.4)	1.18, d (7.6)
17b	5.57, brs				
18	1.15, s	1.42, s	1.67, s	1.09, s	1.08, s
19	0.97, s	4.80, d (11.2)	4.75, d (10.8)	1.11, s	0.92, s
		4.47, d (11.2)	4.70, d (10.8)		
20a	4.15, overlap	4.20, d (10.9)	4.15, d (8.0)	4.21, overlap	
20b		4.09, d (10.9)	3.90, d (8.0)	4.14, overlap	
OAc	2.03, s				
	2.09, s				

^aRecorded in C₅D₅N. ^bRecorded at 400 MHz. ^cRecorded at 500 MHz.

Table 4. ¹³C NMR Spectroscopic Data for Isorosthins F–J (δ in ppm)

position	6 ^{a,b}	7 ^{a,b}	8 ^{a,c}	9 ^{a,c}	10 ^{a,c}
1	28.7, CH ₂	64.3, CH	66.5, CH	31.7, CH ₂	29.2, CH ₂
2	18.8, CH ₂	27.3, CH ₂	31.3, CH ₂	16.0, CH ₂	19.3, CH ₂
3	41.1, CH ₂	28.5, CH ₂	71.5, CH	41.9, CH ₂	40.9, CH ₂
4	34.1, C	39.6, C	43.2, C	34.4, C	34.3, C
5	60.7, CH	57.0, CH	52.7, CH	59.9, CH	55.7, CH
6	74.6, CH	73.4, CH	73.6, CH	73.6, CH	71.9, CH
7	96.9, C	98.5, C	96.4, C	100.6, C	108.2, C
8	62.4, C	61.8, C	60.1, C	56.0, C	55.4, C
9	55.3, CH	47.9, CH	46.6, CH	51.2, CH	42.6, CH
10	37.8, C	40.9, C	41.6, C	37.5, C	44.6, C
11	64.5, CH	15.3, CH ₂	16.0, CH ₂	61.2, CH	16.6, CH ₂
12	37.4, CH ₂	19.4, CH ₂	19.3, CH ₂	33.9, CH ₂	20.3, CH ₂
13	41.6, CH	37.9, CH	31.3, CH	36.9, CH	36.2, CH
14	74.1, CH	74.6, CH	29.3, CH ₂	77.6, CH	76.0, CH
15	207.3, C	225.4, C	226.8, C	71.8, CH	70.7, CH
16	150.1, C	45.6, CH	51.5, CH	44.4, CH	42.7, CH
17	120.6, CH ₂	10.5, CH ₃	10.4, CH ₃	12.0, CH ₃	11.7, CH ₃
18	33.1, CH ₃	27.2, CH ₃	21.8, CH ₃	33.6, CH ₃	31.3, CH ₃
19	22.2, CH ₃	66.6, CH ₂	67.3, CH ₂	22.9, CH ₃	21.2, CH ₃
20	66.5, CH ₂	66.7, CH ₂	66.3, CH ₂	66.8, CH ₂	175.7, C
OAc	21.6, CH ₃	20.8, CH ₃	20.6, CH ₃		
	169.9, C	170.9, C	170.8, C		
	21.3, CH ₃				
	169.7, C				

^aRecorded in C₅D₅N. ^bRecorded at 400 MHz. ^cRecorded at 500 MHz.

and revealed that the double bond in rabdoternin A is reduced in **10**. The structure of **10** was then verified using various 2D-

NMR experiments. In the ROESY spectrum, correlations from H-6 to H₃-19α, H-14 to H-12α, H-15 to H-13α, and H-16 to

Table 5. ¹H NMR Spectroscopic Data for Isorosthins K–P (11–16) (δ in ppm, J in Hz)

position	11 ^{a,c}	12 ^{a,b}	13 ^{a,c}	14 ^{a,b}	15 ^{a,b}	16 ^{a,b}
1a	4.20, m	4.14, m	3.63, m	3.56, m	3.59, m	4.67, brs
2a	1.86, m	1.89–1.78, overlap	2.25, m	1.91, m	1.91, m	1.89, m
2b			1.75, m	1.78, m		
3a	1.39, m	1.42, m	1.42, overlap	1.45, overlap	1.38–1.35, overlap	2.26, m
3b	1.30, m	1.32, m	1.25, overlap	1.32, overlap		1.12, m
5	2.27, d (7.5)	1.86, overlap	1.65, d (8.0)	1.48, overlap	1.46, overlap	2.69, s
6	4.41, m	4.49, overlap	4.43, d (8.0)	4.12, m	4.12, m	
9			1.93, m	1.98, m	2.00, m	2.63, overlap
11a	6.22, brs	6.27, overlap	2.22, m	2.80, m	2.83, m	2.93, m
11b			2.16, m	2.15, m	2.15, m	2.68, overlap
12a	2.78, dd (17.5, 3.5)	2.67, d (18.0)	2.37, m	2.43, m	2.40, m	2.43, m
12b	2.40, d (17.5)	2.14, dd (18.0, 2.1)	1.62, overlap	1.48, overlap	1.40, overlap	1.63, m
13	3.05, d (3.5)	3.04, brs	3.14, d (8.5)	3.26, d (10.0)	3.26, d (10.0)	3.19, d (9.3)
14a	5.89, d (3.5)	2.78, dd (11.0, 4.9)	5.25, brs	5.59, brs	5.60, brs	5.97, brs
14b		2.22, d (11.0)				
15	4.99, s					
17a	5.68, s	6.07, s	6.27, s	6.22, s	6.23, s	6.19, s
17b	5.35, s	5.48, s	5.49, s	5.46, s	5.47, s	5.34, s
18	1.28, s	1.37, s	1.42, s	1.23, s	1.24, s	1.40, s
19	1.17, s	1.18, s	1.38, s	1.03, s	1.06, s	0.95, s
20a	4.61, d (8.5)	4.60, d (8.6)	5.64, s	5.70, s	5.71, s	4.68, s
20b	4.54, d (8.5)	4.50, d (8.6)				
HO-1	5.92, s					
HO-6	8.00, s					
HO-7	8.27, s	9.05, s				
HO-14	6.77, s					
OEt/ OBu			3.65, m; 4.02, m; and 1.10, t	3.56, m; 3.99, m; and 1.09, t	3.46, m; 4.01, m; 1.46, overlap; 1.21, overlap; and 0.73, t (7.4)	

^aRecorded in C₅D₃N. ^bRecorded at 400 MHz. ^cRecorded at 500 MHz.

H-12 α revealed H-6, H-14, H-15, and H-16 as all α -oriented. Compound **10** was characterized, therefore, as 6 β ,7 β ,14 β ,15 β -tetrahydroxy-7 α ,20-olide-*ent*-kaurane.

Compound **11** gave the molecular formula C₂₀H₂₈O₆. The NMR data indicated it to be also a 7,20-epoxy-*ent*-kauranoid with two double bonds in the structure (Tables 5 and 6). One was established as a terminal double bond, and the other placed between C-9 and C-11 by HMBC correlations, from H-11 (δ_{H} 6.22) to C-10 (δ_{C} 44.2) and C-8 (δ_{C} 56.4) and from H-13 (δ_{H} 3.05) to C-11 (δ_{C} 117.9) (Figure 6). In addition, HMBC correlations from H₂-20 and H-3 (δ_{H} 1.39 and 1.30) to C-1 (δ_{C} 71.4), H-6 (δ_{H} 4.41) to C-8, H-12 (δ_{H} 2.78 and 2.40) to C-14 (δ_{C} 79.0), and H₂-17 (δ_{H} 5.68 and 5.35) to C-15 (δ_{C} 79.8) supported the connectivity of the OH groups to C-1, C-6, C-14, and C-15, respectively (Figure 6). The relative configuration of **11** was confirmed by a ROESY experiment, in which correlations of H-1/H-5 β , H-6/H₃-19 α , H-14/H-20b, and H-15/H-13 α revealed H-1, H-6, H-14, and H-15 as being β -, α -, α -, and α -oriented, respectively (Figure 6). As a result, **11** was assigned as 1 α ,6 β ,7 β ,14 β ,15 β -pentahydroxy-7 α ,20-epoxy-*ent*-kaur-9(11),16-diene.

Comparison of the NMR data of **12** with those of isoadenolin I indicated a close structural similarity between these two compounds (Tables 5 and 6).²⁹ Compound **12** was found to differ from isoadenolin I in the replacement of the C-1 OAc group by an OH group. The ROESY experiment

confirmed that **12** displays the same configuration as isoadenolin I. Accordingly, compound **12** was assigned as 1 α ,6 β ,7 β -trihydroxy-7 α ,20-epoxy-*ent*-kaur-9(11),16-dien-15-one.

Compounds **13** and **14** gave the same molecular formula, C₂₂H₃₂O₇, on the basis of HRESIMS. Their NMR data (Tables 5 and 6) indicated the presence of an OEt group in both **13** and **14**. With the help of ¹H–¹H COSY, HSQC, and HMBC spectra, the same planar structure, 20-ethoxy-1,6,7,14-tetrahydroxy-7 α ,20-epoxy-*ent*-kaur-16-en-15-one, was determined for these two compounds. ROESY correlations showed that the difference between these two compounds was the configuration of C-20. In the ROESY spectrum of **13**, H-20 correlated to H-11 α and H-14 α , suggesting the *R** configuration of C-20, while the *S** configuration of C-20 in **14** was determined by the correlations from H-20 to H₃-19 α and H-2 α (Figure 7). The relative configurations of H-1, H-6, and H-14 in **13** and **14** were determined as being β -, α -, and α -oriented by correlations of H-1/H-5 β /H-9 β , H-6/H₃-19 α , and H-14/H-11 α /H-13 α , respectively. Therefore, **13** was assigned as 20(*R**)-20-ethoxy-1 α ,6 β ,7 β ,14 β -tetrahydroxy-7 α ,20-epoxy-*ent*-kaur-16-en-15-one and **14** as 20(*S**)-20-ethoxy-1 α ,6 β ,7 β ,14 β -tetrahydroxy-7 α ,20-epoxy-*ent*-kaur-16-en-15-one.

The HRESIMS of compound **15** suggested the molecular formula of C₂₄H₃₆O₇, indicative of seven degrees of unsaturation. Compound **15** differed from **14** in that the

Table 6. ^{13}C NMR Spectroscopic Data for Isorosthins K–P (11–16) (δ in ppm)

position	11 ^{a,b}	12 ^{a,d}	13 ^{a,c}	14 ^{a,d}	15 ^{a,c}	16 ^{a,d}
1	71.4, CH	72.0, CH	74.2, CH	75.7, CH	75.3, CH	63.4, CH
2	29.9, CH ₂	29.6, CH ₂	30.9, CH ₂	31.4, CH ₂	31.0, CH ₂	28.5, CH ₂
3	39.6, CH ₂	40.4, CH ₂	40.1, CH ₂	39.8, CH ₂	39.5, CH ₂	33.7, CH ₂
4	34.0, C	34.2, C	33.2, C	33.9, C	34.1, C	33.8, C
5	51.5, CH	52.9, CH	59.1, CH	60.4, CH	60.1, CH	59.8, CH
6	74.1, CH	76.0, CH	74.7, CH	75.0, CH	74.7, CH	212.3, C
7	100.6, C	97.4, C	100.1, C	100.1, C	99.7, C	90.9, C
8	56.4, C	62.0, C	63.0, C	62.6, C	62.2, C	60.3, C
9	144.1, C	144.5, C	56.7, CH	54.0, CH	53.7, CH	56.5, CH
10	44.2, C	45.4, C	45.3, C	44.8, C	43.7, C	51.1, C
11	117.9, CH	119.6, CH	21.7, CH ₂	23.8, CH ₂	23.4, CH ₂	20.5, CH ₂
12	39.3, CH ₂	36.3, CH ₂	31.3, CH ₂	31.7, CH ₂	31.3, CH ₂	33.7, CH ₂
13	47.9, CH	37.0, CH	43.5, CH	44.0, CH	44.4, CH	43.6, CH
14	79.0, CH	32.9, CH ₂	72.9, CH	74.2, CH	73.8, CH	74.2, CH
15	79.8, CH	204.4, C	208.4, C	210.9, C	210.3, C	205.2, C
16	150.1, C	153.2, C	153.6, C	153.8, C	153.4, C	153.3, C
17	109.3, CH ₂	118.1, CH ₂	119.5, CH ₂	119.2, CH ₂	118.8, CH ₂	117.0, CH ₂
18	33.9, CH ₃	34.8, CH ₃	36.0, CH ₃	34.5, CH ₃	33.5, CH ₃	35.4, CH ₃
19	23.0, CH ₃	24.1, CH ₃	23.2, CH ₃	22.6, CH ₃	22.3, CH ₃	24.6, CH ₃
20	69.3, CH ₂	68.4, CH ₂	99.4, CH	102.4, CH	102.3, CH	82.0, CH
OEt/OBu			63.7, CH ₂	64.8, CH ₂	68.8, CH ₂	
			15.4, CH ₃	15.8, CH ₃	32.0, CH ₂	
					19.7, CH ₂	
					13.8, CH ₃	

^aRecorded in C₅D₅N. ^bRecorded at 400 MHz. ^cRecorded at 500 MHz. ^dRecorded at 600 MHz.

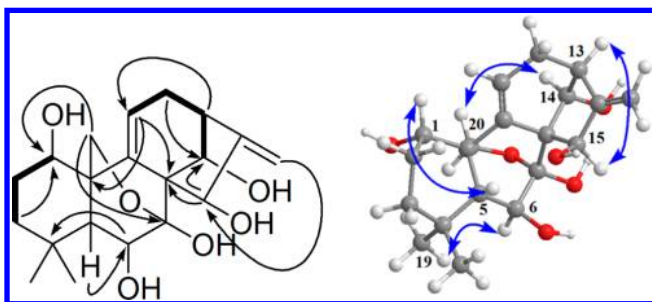


Figure 6. ^1H – ^1H COSY (bold), selected HMBC (arrows), and key ROESY correlations of **11**.

OBu group is replaced with the OEt group located at C-20, as indicated by 1D- and 2D-NMR experiments. Moreover, the same configuration as **14** was determined from the ROESY spectrum. Thus, **15** was elucidated as 20(*S*^{*})-20-*n*-butoxy-1 α ,6 β ,7 β ,14 β -tetrahydroxy-7 α ,20-epoxy-*ent*-kaur-16-en-15-one.

The molecular formula of **16** was determined as C₂₀H₂₆O₆ by HRESIMS. The ^{13}C NMR and DEPT spectra (Table 6) showed typical signals of a 7,20-cyclo-*ent*-kauranoid isolated from the genus *Isodon*.^{30,31,33} Analysis of the HSQC, HMBC, and ^1H – ^1H COSY spectra led to the assignment of the planar structure of **16** as 1,7,14,20-tetrahydroxy-7,20-cyclo-kaur-16-ene-6,15-dione. Comparison the NMR data of **16** with those of rubescensin D, a compound having the same planar structure,³⁰ showed some differences. Detailed analysis of the ROESY spectrum helped distinguish **16** from rubescensin D, since correlations from H-14 to H-12 α confirmed H-14 as being α -oriented, while the 20*S*^{*} configuration of **16** was verified by a correlation between H-20 and H₃-19 α . The only difference between **16** and rubescensin D was the configuration of H-1. Correlations from H-1 to H-20 and H-11 α verified H-1 in **16** as being α -oriented. Therefore, **16** was assigned as 20(*S*^{*})-1 β ,7 β ,14 β ,20-tetrahydroxy-7,20-cyclo-kaur-16-ene-6,15-dione.

All isolates, except compounds **1**, **5**, **14**, and **16** due to sample quantity limitations, were evaluated for their cytotoxic activity against five human cancer cell lines (HL-60, SMMC-

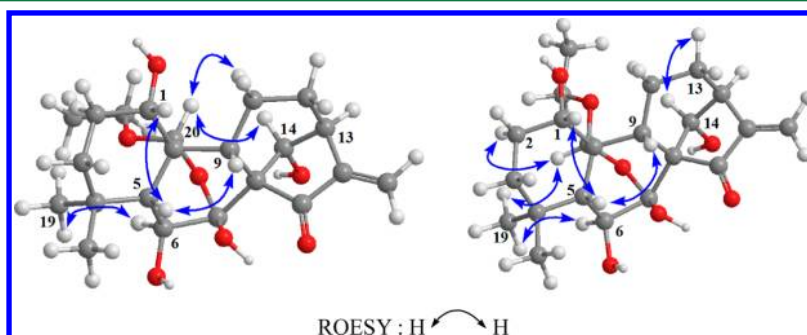


Figure 7. Key ROESY correlations of **13** and **14**.

7721, A-549, MCF-7, and SW-480) using a previously described protocol (Table 7).³⁴ Among these, compounds 4,

Table 7. IC₅₀ Values (μM) of Diterpenoids from *I. rosthornii* for Their Growth Inhibitory Effects on Human Tumor Cell Lines

compound ^a	HL-60	SMMC-7721	A-549	MCF-7	SW480
4	4.3	>10	>10	3.5	3.3
6	4.6	>10	>10	>10	3.2
12	8.8	3.5	4.6	3.3	3.4
13	5.9	>10	>10	8.4	7.8
15	1.2	3.2	3.9	2.6	2.8
17	6.1	>10	>10	>10	>10
18	3.5	4.5	8.6	5.1	2.5
19	1.8	2.7	6.7	2.5	2.4
20	2.5	>10	>10	>10	>10
21	7.9	5.9	5.6	4.2	3.2
23	7.0	>10	>10	>10	9.4
24	2.6	>10	>10	>10	4.1
25	5.3	>10	>10	>10	>10
26	1.5	2.6	3.4	1.8	2.0
cisplatin ^b	2.0	16.2	17.5	17.8	12.8
paclitaxel ^b	<0.008	<0.008	1.4	<0.008	0.04

^aCompounds 2, 3, 7–11, and 23 were inactive (IC₅₀ > 10 μM) for all cell lines. ^bPositive control substance.

6, 13, 17, 20, and 23–25 showed some cytotoxic potency, while compounds 12, 15, 18, 19, 21, and 26 exhibited significant activity (IC₅₀ < 10 μM) for all five cell lines used. The above results suggest that a carbonyl conjugated with the exocyclic double bond group is a structural requirement,¹ and the improvement of lipid solubility may help promote cytotoxic activity. However, it is of interest that some compounds without an exocyclic double bond group like 4 also showed cytotoxic activity.

Inflammation is a systemic response aimed to decrease the toxicity of harmful agents and repair damaged tissue. A key feature of the inflammatory response is the activation of phagocytic cells involved in host defenses. NO, the free radical produced by the inducible NO synthase (iNOS) isoform, is an essential component of the host innate immune and inflammatory responses to a variety of pathogens. Considering the folkloric use of *I. rosthornii*, all isolates except compounds 1, 5, 14, and 16 were tested for their inhibitory activity against NO production in LPS-stimulated RAW264.7 cells. Compounds 4, 12, 13, 15, 17, and 18–26 (Table 8) exhibited some inhibitory activity, and among these, compounds 4, 12, 15, 18, 19, and 26 showed potent inhibitory activity against NO production. The viability of RAW264.7 cells was determined using an MTS assay. At the highest concentration used, none of the tested compounds had any obvious cytotoxicity toward RAW264.7 cells, which suggests that the inhibitory activities against NO production in LPS-stimulated RAW264.7 cells were not induced by the cytotoxicity of the compounds evaluated. These results further support the use of *I. rosthornii* as a Chinese folk therapy.

EXPERIMENTAL SECTION

General Experimental Procedures. Melting points were obtained on an XRC-1 apparatus and are uncorrected. Optical rotations were measured on Horiba SEPA-300 and JASCO P-1020 polarimeters, respectively. UV spectra were obtained using a Shimadzu

Table 8. Inhibitory Effects of the Diterpenoids from *I. rosthornii* on LPS-Activated NO Production in RAW264.7 Cells^a

compound	IC ₅₀ (μM)	compound	IC ₅₀ (μM)
2	>25	17	2.0
3	>25	18	1.7
4	1.5	19	1.9
6	6.3	20	5.2
7	>25	21	3.4
8	>25	22	6.1
9	>25	23	>25
10	>25	24	2.3
11	>25	25	>25
12	2.0	26	1.1
13	3.9	MG-132 ^b	0.10
15	1.5		

^aEach value represents the mean ± SEM (n = 3). ^bPositive control substance.

UV-2401A spectrophotometer. A Tenor 27 spectrophotometer was used for scanning IR spectroscopy with KBr pellets. 1D- and 2D-NMR spectra were recorded on Bruker AM-400, DRX-500, and DRX-600 spectrometers with TMS as internal standard. Unless otherwise specified, chemical shifts (δ) were expressed in ppm with reference to the solvent signals. HRESIMS was performed on an API QSTAR time-of-flight spectrometer. HSCCC was performed on a TBE-300B instrument (TAUTO, Shanghai, People's Republic of China). Semipreparative HPLC was performed on an Agilent 1100 HPLC with a Zorbax SB-C₁₈ (9.4 mm × 25 cm) column. Column chromatography was performed with silica gel (200–300 mesh, Qingdao Marine Chemical, Inc., Qingdao, People's Republic of China), Lichroprep RP-18 gel (40–63 μm, Merck, Darmstadt, Germany), and MCI gel (75–150 μm, Mitsubishi Chemical Corporation, Tokyo, Japan). Fractions were monitored by TLC, and spots were visualized by heating silica gel plates sprayed with 5% H₂SO₄ in EtOH.

Plant Material. The aerial parts of *I. rosthornii* were collected at Daozuo, Qionglai City, Sichuan Province, People's Republic of China, in July 2008, and identified by Prof. Xi-Wen Li, Kunming Institute of Botany. A voucher specimen (KIB 200809003) has been deposited in the Herbarium of the Kunming Institute of Botany, Chinese Academy of Sciences.

Extraction and Isolation. The aerial parts (10 kg) of *I. rosthornii* were extracted with 70% aqueous acetone (20 L) four times (two days each time) at room temperature and filtered. The filtrate was evaporated in vacuo. Then the concentrate without acetone (7 L) was partitioned between EtOAc and H₂O. The EtOAc-soluble portion (485 g) was subjected to silica gel CC (2000 g, 100–200 mesh). Five fractions were produced from the silica gel column, eluting with CHCl₃–Me₂CO (1:0–0:1 gradient system), and were each decolorized on MCI gel, eluted with 90% MeOH–H₂O, to yield fractions A–F.

Fraction B (47 g), a brown gum, was subjected to CC on silica gel (200–300 mesh) and eluted with petroleum ether–Me₂CO (1:0–0:1 gradient), to provide four fractions, B1–B4. Glaucoactone (400 mg) was precipitated from fractions B2, B4, and B5, respectively. After purification by HSCCC (CHCl₃–MeOH–H₂O, 4:3:2) and then by CC (silica gel, petroleum ether–Me₂CO, 9:1–2:1 gradient system), fraction B1 afforded isorosthin B (2, 15 mg). Fraction B2 was separated by HSCCC (CHCl₃–MeOH–H₂O, 4:3:2) and then by preparative and semipreparative HPLC with 53% MeOH–H₂O, to provide isorosthin C (3, 10 mg), 15α-hydroxy-6,7-*seco*-1α,7:11α,6-diolide-20-*al-ent*-kaur-16-ene (17, 40 mg), isodonhenrin B (7 mg), isorosthin D (4, 5 mg), 15α,20β-dihydroxy-6,20-epoxy-1,7-*olide-ent*-kaur-16-ene (12 mg), and 7α,20-epoxy-6β,11β-dihydroxy-7β,14β-[(1-methylethylidene)-bis-oxy]-*ent*-kaur-16-en-15-one (26, 6 mg).

Fraction C (63 g) was separated over RP-18 (MeOH–H₂O gradient system: 30:70–100:0) into four fractions, C1–C4. After further treatment using HSCCC (CHCl₃–MeOH–H₂O, 4:3:2) and column chromatography (silica gel, CHCl₃–Me₂CO, 30:1–10:1), fraction C1 afforded effusanin A (**21**, 12 mg) and 6 α ,15 α -dihydroxy-20-aldehyde-6,7-*seco*-6,11 α -epoxy-1,7-olide-*ent*-kaur-16-ene (**7** mg). Fraction C2 was separated by HSCCC (CHCl₃–MeOH–H₂O, 4:3:2) and then by semipreparative HPLC with 50% MeOH–H₂O to yield isorosthin A (**1**, 2 mg), sculponeatin E (20 mg), isorosthin E (**5**, 2 mg), and isorosthin F (**6**, 5 mg). In the same way, isorosthin L (**12**, 2.5 mg) was isolated from fraction C3, and isorosthinon G (**7**, 12 mg), isorosthin H (**8**, 3 mg), and isorosthin I (**9**, 7 mg) were isolated from fraction C4.

Fraction D (85 g) was separated over RP-18 (MeOH–H₂O gradient system: 30:70–80:20) into fractions D1–D5. Rabdoternin B (**22**, 5.2 g) crystallized from all these fractions. The mother liquor of D1 was first separated by HSCCC (CHCl₃–MeOH–H₂O, 4:3:2) and then was passed through a silica gel column, eluted with CHCl₃–Me₂CO (30:1–1:1) and then by semipreparative HPLC eluted with 45% MeOH–H₂O to yield longikaurin G (**18**, 18 mg) and lasiokaurin (**19**, 50 mg). In the same way, isorosthin O (**15**, 5 mg), rosthornin A (100 mg), rabdoternin A (50 mg), rubescensin D (44 mg), and phyllostachysin A (7 mg) were isolated from fraction D2, and isorosthin M (**13**, 4 mg), isorosthin N (**14**, 1 mg), isorosthin J (**10**, 8 mg), isorosthin P (**16**, 2 mg), rabdoternin F (**23**, 11 mg), and rabdoternin E (**24**, 8 mg) were isolated from fractions D3 and D4.

Fraction E was separated over RP-18 (MeOH–H₂O gradient system: 30:70–80:20), HSCCC (CHCl₃–MeOH–H₂O, 4:3:2), and then by semipreparative HPLC (39% MeOH–H₂O), to give isorosthin K (**11**, 3 mg), isodonol (**20**, 8 mg), lasiokanrinol (10 mg), hebeirubescensin H (3 mg), isoadenolin E (9 mg), and rubescensin O (**25**, 4 mg).

Isorosthin A (1): white, amorphous powder; $[\alpha]_D^{27}$ –140 (c 0.06, MeOH); UV (MeOH) λ_{\max} (log ϵ) 254 (2.28) nm; IR (KBr) ν_{\max} 3432, 2919, 1724, 1630 cm⁻¹; ¹H and ¹³C NMR data, see Tables 1 and 2; positive-ion ESIMS m/z 371 [M + Na]⁺ (100); positive-ion HRESIMS [M + Na]⁺ m/z 371.1481 (calcd for C₁₉H₂₄O₆Na, 371.1470).

Isorosthin B (2): colorless needle crystals (petroleum ether–acetone, 1:1); mp 262–264 °C; $[\alpha]_D^{19}$ –325 (c 0.19, MeOH); UV (MeOH) λ_{\max} (log ϵ) 240 (2.70) nm; IR (KBr) ν_{\max} 3473, 2967, 1740, 1674 cm⁻¹; ¹H and ¹³C NMR data, see Tables 1 and 2; positive-ion ESIMS m/z 425 [M + Na]⁺; positive-ion HRESIMS [M + Na]⁺ m/z 425.1578 (calcd for C₂₂H₂₆O₇Na, 425.1576).

Isorosthin C (3): colorless needle crystals (MeOH); mp 163–165 °C; $[\alpha]_D^{18}$ –140 (c 0.07, MeOH); UV (MeOH) λ_{\max} (log ϵ) 201 (3.08) nm; IR (KBr) ν_{\max} 3436, 2925, 1746, 1628 cm⁻¹; ¹H and ¹³C NMR data, Tables 1 and 2; positive-ion ESIMS m/z 443 [M + Na]⁺; positive-ion HRESIMS [M + Na]⁺ m/z 443.2042 (calcd for C₂₃H₃₂O₇Na, 443.2045).

Isorosthin D (4): white, amorphous powder; $[\alpha]_D^{19}$ –126 (c 0.05, MeOH); UV (MeOH) λ_{\max} (log ϵ) 202 (2.99) nm; IR (KBr) ν_{\max} 3450, 2936, 1737, 1664, 1640 cm⁻¹; ¹H and ¹³C NMR data, see Tables 1 and 2; positive-ion ESIMS m/z 459 [M + Na]⁺; positive-ion HRESIMS [M + Na]⁺ m/z 459.1983 (calcd for C₂₃H₃₂O₈Na, 459.1994).

Isorosthin E (5): white, amorphous solid; $[\alpha]_D^{15}$ –1.60 (c 0.04, MeOH); UV (MeOH) λ_{\max} (log ϵ) 202 (2.64) nm; IR (KBr) ν_{\max} 3424, 2926, 1630, 942 cm⁻¹; ¹H and ¹³C NMR data, see Tables 1 and 2; positive-ion ESIMS m/z 417 [M + Na]⁺; positive-ion HRESIMS [M + Na]⁺ m/z 417.1880 (calcd for C₂₁H₃₀O₇Na, 417.1889).

Isorosthin F (6): white, amorphous powder; $[\alpha]_D^{19}$ –42.1 (c 0.04, MeOH); UV (MeOH) λ_{\max} (log ϵ) 236 (2.69) nm; IR (KBr) ν_{\max} 3408, 2949, 2872, 1737, 1644 cm⁻¹; ¹H and ¹³C NMR data, see Tables 3 and 4; positive-ion ESIMS m/z 471 [M + Na]⁺; positive-ion HRESIMS [M + Na]⁺ m/z 471.1991 (calcd for C₂₄H₃₂O₈, 471.1994).

Isorosthin G (7): white, amorphous powder; $[\alpha]_D^{14}$ –105 (c 0.15, MeOH); UV (MeOH) λ_{\max} (log ϵ) 201 (2.55) nm; IR (KBr) ν_{\max} 3421, 2930, 1713 cm⁻¹; ¹H and ¹³C NMR data, see Tables 3 and 4;

positive-ion ESIMS m/z 447 [M + Na]⁺; positive-ion HRESIMS [M + Na]⁺ m/z 447.2008 (calcd for C₂₂H₃₂O₈Na [M + Na]⁺, 447.1994).

Isorosthin H (8): white, amorphous powder; $[\alpha]_D^{27}$ –141 (c 0.10, MeOH); UV (MeOH) λ_{\max} (log ϵ) 207 (3.15) nm; IR (KBr) ν_{\max} 3473, 3360, 3281, 2938 cm⁻¹; ¹H and ¹³C NMR data, see Tables 3 and 4; positive-ion ESIMS m/z 447 [M + Na]⁺; positive-ion HRESIMS [M + Na]⁺ m/z 447.1990 (calcd for C₂₂H₃₂O₈Na [M + Na]⁺, 447.1994).

Isorosthin I (9): white, amorphous powder; $[\alpha]_D^{14}$ –36.2 (c 0.10, MeOH); UV (MeOH) λ_{\max} (log ϵ) 201 (2.61) nm; IR (KBr) ν_{\max} 3444, 2933, 1632 cm⁻¹; ¹H and ¹³C NMR data, see Tables 3 and 4; positive-ion ESIMS m/z 391 [M + Na]⁺; positive-ion HRESIMS [M + Na]⁺ m/z 391.2092 (calcd for C₂₀H₃₂O₆Na [M + Na]⁺, 391.2096).

Isorosthin J (10): white, amorphous powder; $[\alpha]_D^{14}$ –42.5 (c 0.11, MeOH); UV (MeOH) λ_{\max} (log ϵ) 200 (2.44) nm; IR (KBr) ν_{\max} 3421, 2960, 1723 cm⁻¹; ¹H and ¹³C NMR data, see Tables 3 and 4; positive-ion ESIMS m/z 389 [M + Na]⁺; positive-ion HRESIMS [M + Na]⁺ m/z 389.1943 (calcd for C₂₀H₃₀O₆Na [M + Na]⁺, 389.1940).

Isorosthin K (11): white, amorphous powder; $[\alpha]_D^{15}$ +23.9 (c 0.06, MeOH); UV (MeOH) λ_{\max} (log ϵ) 255 (2.15) nm; IR (KBr) ν_{\max} 3373, 2930, 1665 cm⁻¹; positive-ion ESIMS m/z 387 [M + Na]⁺; ¹H and ¹³C NMR data, see Tables 5 and 6; positive-ion HRESIMS [M + Na]⁺ m/z 387.1782 (calcd for C₂₀H₂₈O₆Na, 387.1783).

Isorosthin L (12): white, amorphous powder; $[\alpha]_D^{26}$ +36.3 (c 0.44, MeOH); UV (MeOH) λ_{\max} (log ϵ) 236 (3.05) nm; IR (KBr) ν_{\max} 3433, 2931, 1713, 1642 cm⁻¹; ¹H and ¹³C NMR data, see Tables 5 and 6; positive-ion ESIMS m/z 369 [M + Na]⁺; positive-ion HRESIMS [M + Na]⁺ m/z 369.1683 (calcd for C₂₀H₂₆O₅Na, 369.1677).

Isorosthin M (13): white, amorphous powder; $[\alpha]_D^{26}$ –47.0 (c 0.18, MeOH); UV (MeOH) λ_{\max} (log ϵ) 237 (3.23) nm; IR (KBr) ν_{\max} 3418, 2926, 2908, 1710, 1644 cm⁻¹; ¹H and ¹³C NMR data, see Tables 5 and 6; positive-ion ESIMS m/z 431 [M + Na]⁺; positive-ion HRESIMS [M + Na]⁺ m/z 431.2047 (calcd for C₂₂H₃₂O₇Na [M + Na]⁺, 431.2045).

Isorosthin N (14): white, amorphous powder; $[\alpha]_D^{26}$ –29.0 (c 0.23, MeOH); UV (MeOH) λ_{\max} (log ϵ) 239 (3.05) nm; IR (KBr) ν_{\max} 3432, 2931, 1711, 1630 cm⁻¹; ¹H and ¹³C NMR data, see Tables 5 and 6; positive-ion ESIMS m/z 431 [M + Na]⁺; positive-ion HRESIMS [M + Na]⁺ m/z 431.2053 (calcd for C₂₂H₃₂O₇Na, 431.2045).

Isorosthin O (15): white, amorphous powder; $[\alpha]_D^{19}$ –49.5 (c 0.04, MeOH); UV (MeOH) λ_{\max} (log ϵ) 238 (2.65) nm; IR (KBr) ν_{\max} 3417, 2931, 1711, 1643 cm⁻¹; ¹H and ¹³C NMR data, see Tables 5 and 6; positive-ion ESIMS m/z 459 [M + Na]⁺; positive-ion HRESIMS [M + Na]⁺ m/z 459.2353 (calcd for C₂₄H₃₆O₇Na [M + Na]⁺, 459.2358).

Isorosthin P (16): white, amorphous powder; $[\alpha]_D^{14}$ –60.7 (c 0.09, MeOH); UV (MeOH) λ_{\max} (log ϵ) 227 (3.17) nm; IR (KBr) ν_{\max} 3454, 2957, 1741, 1648 cm⁻¹; ¹H and ¹³C NMR data, see Tables 5 and 6; negative-ion ESIMS m/z 361 [M – H]⁻; negative-ion HRESIMS [M – H]⁻ m/z 361.1655 (calcd for C₂₀H₂₅O₆ [M – H]⁻, 361.1651).

X-ray Crystal Structure Analysis. Colorless crystals of **2** were obtained in a mixed solvent system of petroleum ether–acetone (1:1), and **3** was obtained in CH₃OH (with three drops of pyridine). Intensity data were collected at 100 K on an Bruker APEX DUO diffractometer equipped with an APEX II CCD, using Mo K α or Cu K α radiation. Cell refinement and data reduction were performed with Bruker SAINT. The structures were solved by direct methods using SHELXS-97.³⁵ Refinements were performed with SHELXL-97 using full-matrix least-squares, with anisotropic displacement parameters used for all the non-hydrogen atoms. The H atoms were placed in the calculated positions and refined using a riding model. Molecular graphics were computed with PLATON. Crystallographic data (excluding structure factor tables) for the structures reported have been deposited with the Cambridge Crystallographic Data Center as supplementary publication no. CCDC 860671 for **2** and CCDC 860672 for **3**. Copies of the data can be obtained free of charge on application to CCDC, 12 Union Road, Cambridge CB 1EZ, UK [fax: Int. +44(0) (1223) 336 033]; e-mail: deposit@ccdc.cam.ac.uk].

Crystallographic data for isorosthin B (2): C₂₂H₂₆O₇, M_w = 402.4, orthorhombic, space group, $P2_12_12_1$, Z = 4, a = 10.800(2) Å, b = 12.432(3) Å, c = 14.828(3) Å; α = β = γ = 90°, V = 1990.9(7) Å³, μ (Mo K α) = 0.100 mm⁻¹, ρ_{calc} = 1.343 g·cm⁻³; S = 1.014, final R

indices: $R_1 = 0.0454$ and $wR_2 = 0.0932$ for 3921 observed from 5503 independent and 20 968 measured reflections ($\theta_{\max} = 30.08$, $I > 2\sigma(I)$ criterion and 267 parameters); maximum and minimum residues are 0.259 and $-0.215 \text{ e} \cdot \text{\AA}^{-3}$, respectively.

Crystallographic data for isorosstin C (3): $\text{C}_{28}\text{H}_{37}\text{NO}_7$ ($\text{C}_{23}\text{H}_{32}\text{O}_7 + \text{C}_5\text{H}_5\text{N}$), $M_w = 499.6$, monoclinic, space group, $P2_1$, $Z = 2$, $a = 10.84840(10) \text{ \AA}$, $b = 10.33650(10) \text{ \AA}$, $c = 11.66760(10) \text{ \AA}$; $\alpha = \gamma = 90.00^\circ$, $\beta = 93.36^\circ$, $V = 1306.11(2) \text{ \AA}^3$, $\mu(\text{Cu K}\alpha) = 0.742 \text{ mm}^{-1}$, $\rho_{\text{calc}} = 1.270 \text{ g} \cdot \text{cm}^{-3}$; $S = 1.035$, final R indices: $R_1 = 0.0271$ and $wR_2 = 0.0722$ for 3760 observed from 3793 independent and 11 102 measured reflections ($\theta_{\max} = 69.43$, $I > 2\sigma(I)$ criterion and 331 parameters); maximum and minimum residues are 0.251 and $-0.163 \text{ e} \cdot \text{\AA}^{-3}$, respectively. The Flack³² parameter value was $x = 0.02(12)$.

Cytotoxicity Assays. The human tumor cell lines HL-60, SMMC-7721, A-549, MCF-7, and SW-480 were used, which were obtained from ATCC (Manassas, VA, USA). All cells were cultured in RPMI-1640 or DMEM medium (Hyclone, Logan, UT, USA), supplemented with 10% fetal bovine serum (Hyclone) at 37°C in a humidified atmosphere with 5% CO_2 . Cell viability was assessed by conducting colorimetric measurements of the amount of insoluble formazan formed in living cells based on the reduction of 3-(4,5-dimethylthiazol-2-yl)-2,5-diphenyltetrazolium bromide (MTT) (Sigma, St. Louis, MO, USA).³⁴ Briefly, $100 \mu\text{L}$ of adherent cells was seeded into each well of a 96-well cell culture plate and allowed to adhere for 12 h before test compound addition, while suspended cells were seeded just before test compound addition, both with an initial density of 1×10^5 cells/mL in $100 \mu\text{L}$ of medium. Each tumor cell line was exposed to each test compound at various concentrations in triplicate for 48 h, with cisplatin and paclitaxel (Sigma) used as positive controls. After incubation, MTT ($100 \mu\text{g}$) was added to each well, and the incubation continued for 4 h at 37°C . The cells were lysed with $100 \mu\text{L}$ of 20% SDS–50% DMF after removal of $100 \mu\text{L}$ of medium. The optical density of the lysate was measured at 595 nm in a 96-well microtiter plate reader (Bio-Rad 680). The IC_{50} value of each compound was calculated by Reed and Muench's method.³⁶

Nitric Oxide Production in RAW 264.7 Macrophages. Murine monocytic RAW264.7 macrophages were dispensed into 96-well plates (2×10^5 cells/well) containing RPMI 1640 medium (Hyclone) with 10% FBS under a humidified atmosphere of 5% CO_2 at 37°C . After 24 h preincubation, cells were treated with serial dilutions of the compounds with the maximum concentration of $25 \mu\text{M}$ in the presence of $1 \mu\text{g}/\text{mL}$ LPS for 18 h. Each compound was dissolved in DMSO and further diluted in medium to produce different concentrations. NO production in each well was assessed by adding $100 \mu\text{L}$ of Griess reagent (reagent A and reagent B, respectively, Sigma) to $100 \mu\text{L}$ of each supernatant from LPS (Sigma)-treated or LPS- and compound-treated cells in triplicate. After 5 min incubation, the absorbance was measured at 570 nm with a 2104 Envision multilabel plate reader (Perkin-Elmer Life Sciences, Inc., Boston, MA, USA). MG-132 was used as a positive control.³⁷

The cytotoxicity of tested compounds was evaluated using an MTS assay.³⁴ Briefly, RAW264.7 cells, 2×10^5 cells/well, were seeded in 96-well plates. After 24 h incubation, cells were treated with or without test compounds at given concentrations for 18 h. Then, MTS was added to each well and the plates were kept for 4 h. Test compounds were dissolved in DMSO, and the absorbance was read at 490 nm. Cytotoxicity was calculated by cell viability of cells without test compounds as 100%.

■ ASSOCIATED CONTENT

■ Supporting Information

Supplementary data associated with this article (^1H , ^{13}C NMR, DEPT, HSQC, HMBC, COSY, NOESY, HRESIMS, IR, and UV spectra of compounds **1**, **2**, **4**, **11**, **13**, and **16** and ^1H , ^{13}C NMR, DEPT, and HRESIMS spectra of compounds **3**, **5–10**, **12**, **14**, and **15**) are available free of charge via the Internet at <http://pubs.acs.org>.

■ AUTHOR INFORMATION

Corresponding Author

*E-mail: pujianxin@mail.kib.ac.cn; hdsun@mail.kib.ac.cn. Tel: (86) 871-5223616. Fax: (86) 871-5216343.

Notes

The authors declare no competing financial interest.

■ ACKNOWLEDGMENTS

This project was supported financially by the National Natural Science Foundation of China (No. 81172939), the Major State Basic Research Development Program of China (No. 2009CB522300), the reservation-talent project of Yunnan Province (2011CI043), the Science and Technology Program of Yunnan Province (No. 2008IF010), the Major Direction Projection Foundation of CAS Intellectual Innovation Project (No. KSCX2-EW-J-24), and West Light Foundation of the Chinese Academy of Sciences (J.-X.P.).

■ REFERENCES

- (1) Sun, H.-D.; Huang, S.-X.; Han, Q.-B. *Nat. Prod. Rep.* **2006**, *23*, 673–698.
- (2) Dao, T.-T.; Lee, K.-Y.; Jeong, H.-M.; Nguyen, P.-H.; Tran, T.-L.; Thuong, P.-T.; Nguyen, B.-T.; Oh, W.-K. *J. Nat. Prod.* **2011**, *74*, 2526–2531.
- (3) Wang, L.; Zhao, W.-L.; Yan, J.-S.; Liu, P.; Sun, H.-P.; Zhou, G.-B.; Weng, Z.-Y.; Wu, W.-L.; Weng, X.-Q.; Sun, X.-J.; Chen, Z.; Sun, H.-D.; Chen, S.-J. *Cell Death Differ.* **2007**, *14*, 306–317.
- (4) Zhang, Y.-W.; Jiang, X.-X.; Chen, Q.-S.; Shi, W.-Y.; Wang, L.; Sun, H.-D.; Shen, Z.-X.; Chen, Z.; Chen, S.-J.; Zhao, W.-L. *Exp. Hematol.* **2010**, *38*, 191–201.
- (5) Xu, H.-Z.; Huang, Y.; Wu, Y.-L.; Zhao, Y.; Xiao, W.-L.; Lin, Q.-S.; Sun, H.-D.; Dai, W.; Chen, G.-Q. *Cell Cycle* **2010**, *9*, 2897–2907.
- (6) Gu, Z.-M.; Wu, Y.-L.; Zhou, M.-Y.; Liu, C.-X.; Xu, H.-Z.; Yan, H.; Zhao, Y.; Huang, Y.; Sun, H.-D.; Chen, G.-Q. *Blood* **2010**, *116*, 5289–5297.
- (7) Fujita, E.; Fujita, T.; Katayama, H.; Shibuya, M. *Chem. Commun.* **1967**, 252–254.
- (8) Fujita, E.; Taoka, M.; Shibuya, M.; Fujita, T.; Shingu, T. *J. Chem. Soc., Perkin Trans. 1* **1973**, 2277–2281.
- (9) Liu, C.-X.; Yin, Q.-Q.; Zhou, H.-C.; Wu, Y.-L.; Pu, J.-X.; Xia, L.; Liu, W.; Huang, X.; Jiang, T.; Wu, M.-X.; He, L.-C.; Zhao, Y.-X.; Wang, X.-L.; Xiao, W.-L.; Chen, H.-Z.; Zhao, Q.; Zhou, A.-W.; Wang, L.-S.; Sun, H.-D.; Chen, G.-Q. *Nat. Chem. Biol.* **2012**, *8*, 486–493.
- (10) Xu, Y.; Ma, Y. *Phytochemistry* **1989**, *28*, 3235–3237.
- (11) Li, G.-Y.; Wang, Y. L. *Yaoyue Xuebao* **1984**, *19*, 590–592.
- (12) Xu, Y.-L.; Li, Z.-Q. *Yunnan Zhiwu Yanjiu* **1998**, *20*, 97–101.
- (13) Ku, I.; Xu, Y.-L. *Phytother. Res.* **2004**, *18*, 180–183.
- (14) Zhan, R.; Du, X.; Su, J.; Li, X.-N.; Wang, W.-G.; Liang, C.-Q.; Yang, J.-H.; Li, Y.; Pu, J.-X.; Sun, H.-D. *Nat. Prod. Bioprospect.* **2011**, *1*, 116–120.
- (15) Zhao, W.; Pu, J.-X.; Du, X.; Wu, Y.-L.; Zhao, Y.; He, F.; Zhang, H.-B.; Xue, Y.-B.; Xiao, W.-L.; Chen, G.-Q.; Sun, H.-D. *Arch. Pharm. Res.* **2011**, *34*, 2007–2014.
- (16) Takeda, Y.; Fujita, T. *Planta Med.* **1988**, *54*, 327–329.
- (17) Fujita, E.; Taoka, M. *Chem. Pharm. Bull.* **1972**, *20*, 1752–1754.
- (18) Sun, H.-D.; Lin, Z.-W.; Niu, F.-D.; Shen, P.-Q.; Pan, L.-T.; Lin, L.-Z.; Cordell, G. A. *Phytochemistry* **1995**, *38*, 1451–1455.
- (19) Fujita, T.; Takeda, Y.; Shingu, T.; Ueno, A. *Chem. Lett.* **1980**, *9*, 1635–1638.
- (20) Fujita, E.; Taoka, M.; Fujita, T. *Chem. Pharm. Bull.* **1974**, *22*, 280–285.
- (21) Takeda, Y.; Takeda, K.; Fujita, T.; Sun, H.; Minami, Y. *Phytochemistry* **1994**, *35*, 1513–1516.
- (22) Han, Q.-B.; Jiang, B.; Zhang, J.-X.; Niu, X.-M.; Sun, H.-D. *Helv. Chim. Acta* **2003**, *86*, 773–777.
- (23) Takeda, Y.; Fujita, T. *Planta Med.* **1988**, *54*, 327–329.

- (24) Yan, F.-L.; Zhang, L.-B.; Zhang, J.-X.; Sun, H.-D. *Chin. Chem. Lett.* **2007**, *18*, 1383–1385.
- (25) Meng, X.; Wang, Q.; Chen, Y. *Phytochemistry* **1989**, *28*, 1163–1165.
- (26) Hu, Z.; Zhan, R.; Du, X.; Su, J.; Li, X.-N.; Yang, J.-H.; Zhang, H.-B.; Li, Y.; Sun, H.-D.; Li, G.-P.; Pu, J.-X. *Chem. Pharm. Bull.* **2011**, *59*, 1562–1566.
- (27) Jiang, B.; Hou, A.-J.; Li, M.-L.; Li, S.-H.; Han, Q.-B.; Wang, S.-J.; Lin, Z.-W.; Sun, H.-D. *Planta Med.* **2002**, *68*, 921–925.
- (28) Huang, S.-X.; Zhou, Y.; Pu, J.-X.; Li, R.-T.; Li, X.; Xiao, W.-L.; Lou, L.-G.; Han, Q.-B.; Ding, L.-S.; Peng, S.-L.; Sun, H.-D. *Tetrahedron* **2006**, *62*, 4941–4947.
- (29) Zhao, W.; Pu, J.-X.; Du, X.; Su, J.; Li, X.-N.; Yang, J.-H.; Xue, Y.-B.; Li, Y.; Xiao, W.-L.; Sun, H.-D. *J. Nat. Prod.* **2011**, *74*, 1213–1220.
- (30) Sun, H.-D.; Zhou, Q.; Fujita, T.; Takeda, Y.; Minami, Y.; Marunaka, T.; Lin, Z.; Shen, X. *Phytochemistry* **1992**, *31*, 1418–1419.
- (31) Fujita, T.; Sun, H.-D.; Takeda, Y.; Minami, Y.; Marunaka, T.; Lin, Z.-W.; Xu, Y.-L. *J. Chem. Soc., Chem. Commun.* **1985**, 1738–1739.
- (32) Flack, H. D. *Acta Crystallogr., Sect. A* **1983**, *A39*, 876–881.
- (33) Li, L.-M.; Li, G.-Y.; Li, S.-H.; Weng, Z.-Y.; Xiao, W.-L.; Han, Q.-B.; Ding, L.-S.; Lou, L.-G.; Sun, H.-D. *Chem. Biodiversity* **2006**, *3*, 1031–1038.
- (34) Monks, A.; Scudiero, D.; Skehan, P.; Shoemaker, R.; Paull, K.; Vistica, D.; Hose, C.; Langley, J.; Cronise, P.; Vaigro-Wolff, A. *J. Natl. Cancer Inst.* **1991**, *83*, 757–766.
- (35) Sheldrick, G.-M.; Schneider, T.-R. *Methods Enzymol.* **1997**, *277*, 319–343.
- (36) Reed, L. J.; Muench, H. *Am. J. Hyg.* **1938**, *27*, 493–497.
- (37) Fan, J.-T.; Su, J.; Peng, Y.-M.; Li, Y.; Li, J.; Zhou, Y.-B.; Zeng, G.-Z.; Yan, H.; Tan, N.-H. *Bioorg. Med. Chem.* **2010**, *18*, 8226–8234.